Numerical and experimental investigation of pressure-swirl nozzles produced by additive manufacturing

Patrick Lüscher[1]*, Janine Bochsler[1], Daniel A. Weiss[1], Marc Huber[2], Kaspar Löffel[2], René van Nieulande[3], Tom Duda[4]
[1]Institute of Thermal and Fluid Engineering, FHNW, Windisch, Switzerland
[2]Institute of Product and Production Engineering, FHNW, Windisch, Switzerland
[3]Emerson Automation Solutions, Breda, Netherlands
[4]Emerson Automation Solutions, Baar, Switzerland
*Corresponding author: patrick.luescher@fhnw.ch

Abstract
Conventionally produced pressure-swirl nozzles suffer from the disadvantage that the geometry is restricted by the manufacturing technique. Modern technologies like metal 3D printing by selective laser melting (SLM) allow for more complex geometries with reduced flow resistance, which can improve overall efficiency. In this paper three nozzles for steam temperature control are investigated, two conventional ones and one designed for additive manufacturing. The goal is to optimize the nozzle to as small droplets as possible at an identical flow rate to achieve a fast evaporation. The different nozzles were investigated using ANSYS CFX 18.2 based on a VOF (Volume of Fluid) approach combined with a RANS turbulence model. As validation, the droplet distributions generated by the three nozzles were measured at a test stand using laser diffraction analysis together with the mass flow rate and the spray angle. The droplet size cannot be determined from the simulations, but mass flow rate and spray angle showed good agreement. Both the simulation as well as the experiments were carried out with water sprayed into ambient air with a pressure difference of 0.61 MPa. For a proper comparison between nozzles with a different throughput, a new way was introduced to estimate the drop size if the nozzle were geometrically scaled to the desired mass flow. To investigate the influence of a higher surface roughness, the conventional nozzles were also produced by SLM and various quantities were compared. As expected, the nozzles with a high surface roughness produce larger droplets, but they also have a higher throughput.

Keywords
Volume of fluid, CFD, pressure-swirl, atomization, additive manufacturing

Introduction

For a safe and efficient operation in combined-cycle power generation facilities the temperature of the steam has to be adjusted precisely. The device to control the steam temperature is called a desuperheater and is placed within the boiler circuit. By injecting water into the stream the device regulates the steam temperature. Due to fluctuations in the process, the desuperheaters have multiple different nozzles for several operation conditions, which are regulated over a valve. Downstream of the desuperheater follows a straight pipe until the evaporation is complete. Therefore a good atomization can reduce pipe length and thereby losses and cost of the system.
The nozzles which are implemented in such a desuperheater today consist of multiple parts and have to be mounted in the sprayhead. Modern technologies like metal 3D printing by selective laser melting (SLM) allow for more complex nozzle geometries without the need to assemble multiple parts. This yields the benefits of a reduced lead time and customized sprayheads while improving the flow in the nozzles and thereby also the atomization.
To maximize the benefits from printing the sprayhead, the design of the nozzles has to be adjusted to the new manufacturing technology. One clear drawback is that the surface roughness of a part produced by SLM is a lot higher than of a conventionally produced part. In the literature no studies have been found which investigate the potential and the optimization of pressure-swirl nozzles produced with additive manufacturing. In the present work three different nozzles were studied by simulation and experiments to explore the potential of 3D printed nozzles. Furthermore, the geometrical scaling of a nozzle was studied to compare them at the same mass flow.

Nozzles investigated

A schematic representation of a pressure-swirl nozzle is shown in Figure 1. The flow enters the swirl chamber ideally tangential to create a swirl, which then causes a steam core due to low pressure in the center. At the orifice the liquid film generates a hollow cone with angle θ, which then decays into droplets.
In this work, three different nozzle types were simulated and measured on the test stand. Nozzle (A) and (B) get produced by conventional methods and consist of three and two parts respectively. Both nozzles get brazed into the sprayhead to guarantee their sealing and they both suffer from the limitations enforced by the manufacturing methods.
Producing a nozzle by SLM gives a lot of possibilities to create a smooth flow path with minimal pressure loss. To do so nozzle (C) was designed according to the values described by Jones [1] with no sharp edges and the inlet

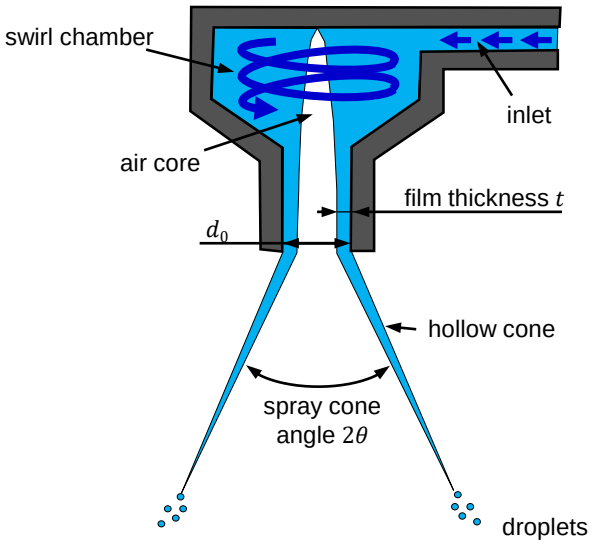

Figure 1. Schematic representation of a pressure-swirl nozzle.

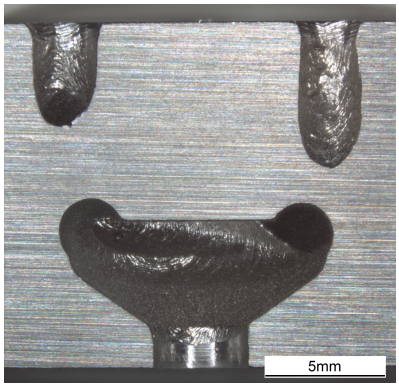

Figure 2. Section through a post-processed nozzle (C).

ports entering the swirl chamber perfectly tangential. Nozzle (A) and (B) were also printed by SLM for comparison, so that the influence of the surface roughness could be investigated.
SLM is a powder bed process, which builds up the object layer by layer. A wiper distributes the metal powder, in this case Inconel 625, equally over the build platform. A laser then melts the powder according to the slice data of the object. Those steps are repeated until the entire part is finished. The powder has an initial size of $15 - 45\,\mu m$, which results in a surface roughness of $R_a = 5 - 25\,\mu m$ depending on the orientation of the respective surface. The build-up direction is perpendicular to the nozzle axis, as the complete sprayhead will also be built in this direction. Because free hanging surfaces are hard to print, this build-up direction yields the disadvantage of an inhomogeneous surface around the circumference. To reach the best possible surface quality the orifice with diameter d_0 gets post-processed after printing. A section of a printed nozzle (C) after post-processing is shown in Figure 2.

Numerical setup

All simulations were carried out with ANSYS CFX 18.2 using a *Volume of Fluid* (VOF) approach to resolve the two phases and the free surface between them. The Reynolds number based on the liquid film at the exit is in the order of 10^5. The flow was therefore assumed turbulent and the *Shear Stress Transport* (SST) turbulence model was used. As the nozzles operate stationary fashion and there are no transient effects to be expected, only steady state solutions were computed.
First, the flow field was initialized with a fixed mass flow at the inlet and constant pressure at the outlet. In a second step the inlet got changed to a constant pressure, so that the pressure difference was identical to the experiments and the results can be compared. No-slip walls, which are hydraulically smooth, were used for all the surfaces.
Even though the real application of those nozzles will be in overheated steam, in the simulations the water got sprayed into air at 20 °C and 0.1 MPa, which are the same conditions as in the laboratory. Like the air, the water was also chosen to be at 20 °C. A parameter study showed that the influence of the chosen temperature and pressure level on all flow properties is negligible.

Geometry and Mesh

Downstream of the nozzle a cylinder with a diameter of 30 mm and a length of 10 mm was added to resolve the hollow spray cone. The mesh in the middle of the nozzle was chosen to be finer than the mesh in the remaining regions to better resolve the air core. The mesh in the downstream cylinder was adapted during the simulation along the free surface of the water to get a good resolution in a reasonable time. Therefore, the mesh got refined in five steps in the cells where the gradient of the volume fraction showed the highest values. During this process the total number of nodes in the whole mesh got more than doubled. A typical mesh for the nozzle (C) after the refinement can be seen in Figure 3.
A detailed mesh study with the nozzle (C) was performed, where the cell size in three different regions was varied. A good compromise between accuracy and computation time in all three regions was chosen and subsequently the mesh refinement in the downstream region was studied. With the same settings for all three nozzles, the mesh for nozzle (A) and (C) ended up having about $3.5 \cdot 10^6$ cells and the mesh for nozzle (B) having about $6.5 \cdot 10^6$ cells.

Evaluation

The resulting liquid volume fraction of the nozzle (C) is shown in Figure 4. One can clearly identify the air core reaching to the back wall of the swirl chamber and also the spray cone downstream of the nozzle. For a quantitative

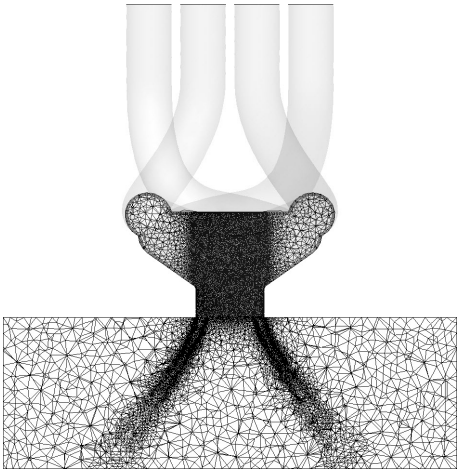

Figure 3. Refined mesh of the nozzle (C).

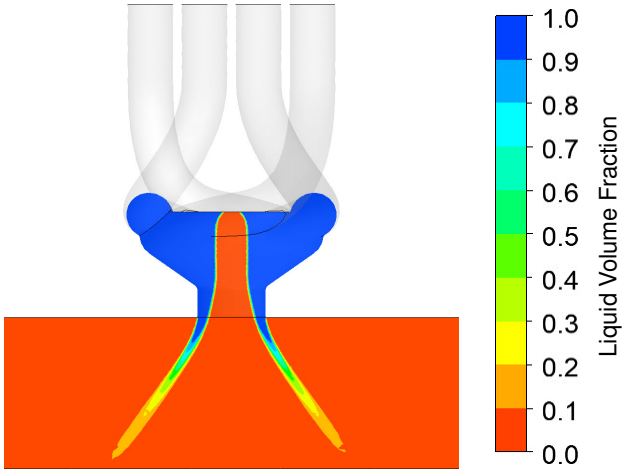

Figure 4. Resulting Volume fraction inside the nozzle (C).

analysis three quantities were calculated from each simulation: The liquid mass flow $\dot{m}$, the spray cone angle θ and the film thickness t. The liquid mass flow can be simply read out from the inlet boundary. Because of a finite resolution and numerical diffusion, the liquid film does not have a clear boundary. Therefore, the average volume fraction X at the exit of the orifice was used to calculate the film thickness with

$$t = \frac{d_0}{2}(1 - \sqrt{1 - X})\,. \tag{1}$$

For the cone angle 1000 streamlines were computed starting from the inlet. The coordinates from all those streamlines were exported and converted to a cylindrical coordinate system. Each streamline was then approximated with a straight line between 2 mm and 10 mm downstream of the nozzle. Averaging the angles of all those lines gave the average spray angle of a nozzle.

Experimental setup

The schematic setup of the test stand is shown in Figure 5. A high-pressure plunger pump with a built-in pressure damper was used to create the water pressure. The pressure could be adjusted with a hand valve, which bypassed most of the water back to the tank. After the bypass valve, the mass flow got measured using a Coriolis flow meter and a safety valve prevented pressures higher than 4.5 MPa. The water got transported through a vertical pipe with a length-to-diameter ratio of 40 to get a fully developed velocity profile. At the bottom of the pipe were a pressure measurement and a flange, to which a second flange with the nozzle could be mounted. To measure the droplet

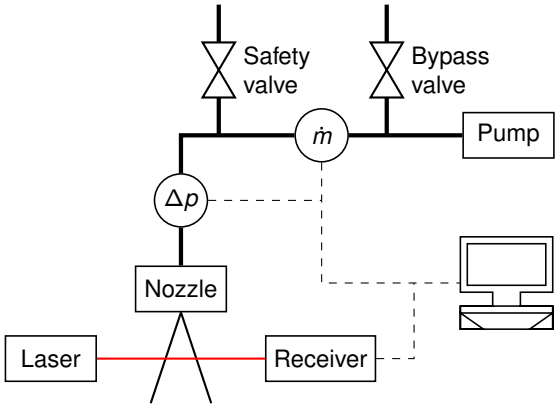

Figure 5. Experimental setup

size a laser diffraction analyser from Malvern Spraytec was used. The analyser setup consisted of a He-Ne laser, a receiver and a processor and was placed 330 mm below the nozzle. The laser light gets scattered depending on the size of the droplets so that the detector can reconstruct the drop size distribution. This method measures all droplets along the laser path, but does not give any information about velocity or volumetric flow rate. As the spray might not be uniform over the whole circumference, measurements were taken and averaged every 45°. The measured volume frequency at one certain angle is shown in Figure 6 (blue) together with the cumulative volume (red). From this measurement the Sauter mean diameter (SMD) was calculated with

$$SMD = \frac{\sum d^3}{\sum d^2} \tag{2}$$

and is displayed with a black line.
In addition to the droplet size the spray angle was also measured. To do so a common digital camera was placed about 1 m away on the same height as the nozzle. A program was written which calculates the angle from four points added to the picture by the user. Figure 7 shows a picture from nozzle Ⓒ with the manual points. As the contour of the spray is not clearly visible, this method has an accuracy of about ±3°, which is sufficient to compare different nozzles among each other.

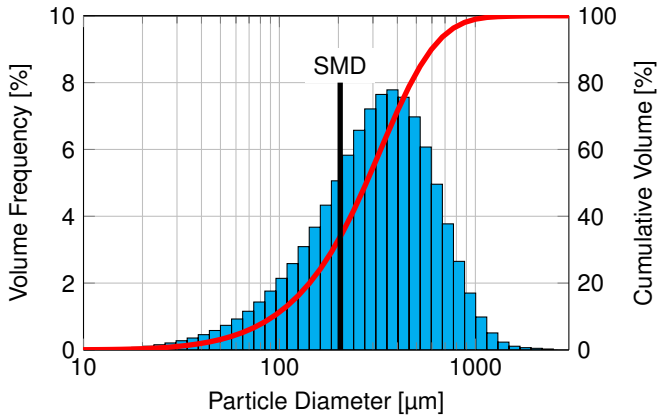

Figure 6. Result of a spray measurement of the nozzle Ⓒ at Δp = 0.61 MPa. Blue is the volume frequency, red is the cumulative volume and black is the resulting SMD.

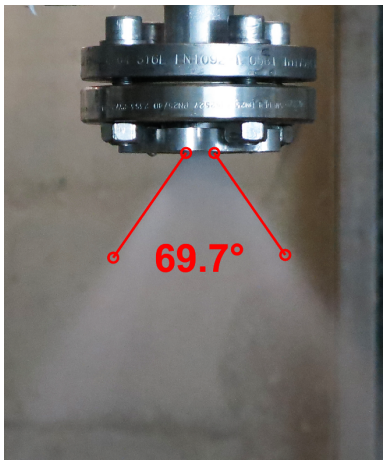

Figure 7. Spray of the nozzle Ⓒ at Δp = 0.61 MPa.

Results and discussion

All simulations and experiments were performed at Δp = 0.61 MPa. However, simulations do not estimate drop sizes, so the SMD could only be compared for the experimental results. On the other hand, the simulations provided a film thickness t and the possibility to further inspect the flow field inside the nozzle.

Scaling

It is delicate to compare droplet diameters of nozzles which result in different mass flows at the same pressure drop. When working with SLM, those nozzles could be simply scaled in order to have the same mass flow. As this process would be too time consuming a simpler way of comparing nozzles with different throughputs had to be found. Because fluid properties, pressure difference and geometric ratios stay constant while scaling, a relationship of the form

$$SMD \sim \dot{m}^x \tag{3}$$

would be ideal. To find the exponent x, several drop size relationships from different studies were conducted.
Wang and Lefebvre [3] derived the following correlation with the assumption that the atomization is a two-stage process

$$SMD = 4.52 \left(\frac{\sigma \mu_L}{\rho_A \Delta p^2}\right)^{0.25} (t \cdot \cos\theta)^{0.25} + 0.39 \left(\frac{\sigma \rho_L}{\rho_A \Delta p}\right)^{0.25} (t \cdot \cos\theta)^{0.75}. \tag{4}$$

Multiple simulations were made with the nozzle Ⓒ scaled between 80% and 120% of the reference. The results show that neither the spray angle θ nor the relative film thickness t/d_0 depend on the size of the nozzle and therefore, the term $(t \cdot \cos\theta)$ is found to be proportional to the exit diameter d_0. With the definition of the discharge coefficient c_D one can write $(t \cdot \cos\theta) \sim \sqrt{\dot{m}}$. Together with the assumptions described before the correlation for the SMD reduces to the form

$$SMD = A \cdot \dot{m}^{0.125} + B \cdot \dot{m}^{0.375} \tag{5}$$

with the two unknowns A and B. Depending on those two constants, the coefficient x must lie between 0.125 and 0.375. Benjamin *et al.* [4] used the same form of correlation to predict the SMD as Wang and Lefebvre [3], but redefined all coefficients with their own measurements. Their findings suggest that the exponent x should be between 0.419 and 0.474. Different studies from Jones [1], Jasuja [5] and Jain *et al.* [6] suggest a coefficient x of 0.315, 0.22 or 0.345 respectively.
Of the mentioned sources only Jones [1] covered the range used in the present study and none of them studied or mentioned the influence of a higher surface roughness. Nevertheless, those correlations give a good indication of the exponent x valid for the nozzles printed by SLM.
Nozzle Ⓒ was produced in five different scales between 45% and 170% of the reference size and then measured at two different pressure differences. The resulting mass flow depending on the scaling is shown in Figure 8. The

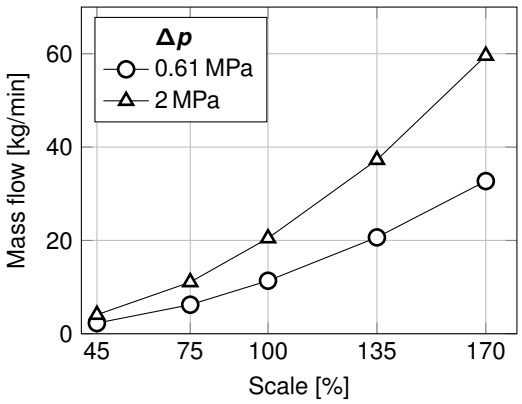

Figure 8. Mass flow of nozzle (C) depending on the scaling at different Δp.

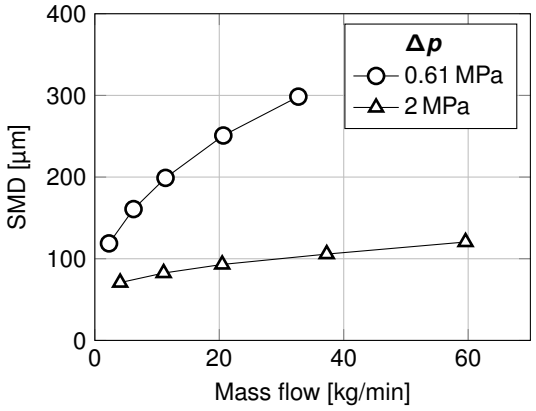

Figure 9. SMD of nozzle (C) depending on the mass flow at different Δp.

curves for both pressures can be fitted with a quadratic function, which corresponds to $\dot{m} \propto d_0^2$. According to Lefebvre [7], the discharge coefficient is defined by

$$c_D = \frac{\dot{m}}{A_0 \cdot \sqrt{2\rho_L \Delta p}} . \tag{6}$$

and should be constant for a given geometry, which is supported by the present measurements. As all nozzles have the same absolute roughness but a different size, this also indicates that the relative roughness has no significant impact on the mass flow.
Figure 9 shows the resulting SMD plotted against the mass flow. Here, the curves were fitted with functions of the form of Equation 3, which results in exponents of 0.359 and 0.204 for 0.61 MPa and 2 MPa respectively. Those values reasonably align with the literature, however the high dependence on the pressure difference was not expected. With this information the measured droplet diameter can be scaled to a common mass flow using

$$SMD^{(2)} = SMD^{(1)} \cdot \left(\frac{\dot{m}^{(2)}}{\dot{m}^{(1)}} \right)^x \tag{7}$$

and the exponent for the respective pressure.

Surface roughness

The most common way to measure surface roughness of a mechanical component is the R_a-value, which is defined as the arithmetic average of the profile along a line. On the other hand, ANSYS CFX works with the sand-grain roughness ε. According to Adams *et al.* [2] the sand grain roughness can be estimated with $\varepsilon = 5.863 \cdot R_a$. Simulations with a sand grain roughness of $\varepsilon = 146.6\,\mu m$, which corresponds roughly to $R_a = 25\,\mu m$, were performed for all three nozzles to investigate its influence. As the surface of a printed nozzle is very inhomogeneous and the correlation by Adams *et al.* has a large uncertainty, the surface roughness is not represented correctly in the simulations. Nevertheless, it can help to show the qualitative trends of a rough surface. The main results of all six simulations are summarized in Table 1.

Table 1. Results of the simulations at $\Delta p = 0.61$ MPa. The *rough* simulations have a sand grain roughness of $\varepsilon = 146.6\,\mu m$.

	smooth			rough		
	$\dot{m}$ [kg/min]	θ [°]	t [µm]	$\dot{m}$ [kg/min]	θ [°]	t [µm]
Nozzle (A)	12.1	37.9	690	12.9	35.7	776
Nozzle (B)	7.5	46.6	774	9.8	42.1	1028
Nozzle (C)	12.9	35.9	746	13.3	34.8	816

Nozzle (A) and (C) showed an increase in film thickness t by about 10% while the spray angle θ decreased by about 5% compared to the hydraulically smooth simulation. Nozzle (B) showed the same trends but much more drastically, which might have been caused by a longer and thinner air core. Wang and Lefebvre [3] showed that a thinner liquid film and a higher spray angle lead to smaller droplets. Therefore, the trends detected in the simulations support the assumption that a high surface roughness results in larger droplets. In return, the mass flow from the rough nozzles was also about $3 - 30\%$ higher than from the smooth nozzles, which puts the larger droplets into perspective. This point is rather counterintuitive, as a higher surface roughness usually leads to a higher pressure loss and therefore to a smaller mass flow.

A closer inspection of the simulation results showed that the rough surface in the inlet ports results in a lower total pressure of the fluid in the swirl chamber. This in turn results in a weaker swirl and therefore a higher film thickness and a smaller spray angle. Even though the swirl chamber also has a higher surface roughness, it is assumed that the weaker swirl leads to a higher mass flow.
As a comparison, all three nozzle types were measured at the test stand and the results are shown in Table 2. Nozzle (C) cannot be produced by conventional methods, so those values are missing. To compare the measured droplet diameters, the SMD was scaled to $\dot{m} = 11.2\,\mathrm{kg/min}$ making use of Equation 7 with an exponent of $x = 0.359$. Even though the film thickness cannot be compared, one can see that the spray angle is also smaller when the surface is rougher. Also, both nozzles produced significantly larger droplets when they were manufactured by SLM instead of conventional methods. Nozzle (B) also supports the theory of a higher mass flow at a higher surface roughness, but nozzle (A) works in the opposite direction: The 3D printed nozzle has a much lower mass flow, which cannot be explained with the theory above. Most likely, this was caused by the unshapely interior after printing as this nozzle was not designed for SLM.

Table 2. Results of the experiments at $\Delta p = 0.61\,\mathrm{MPa}$. Droplet diameters are scaled to $\dot{m} = 11.2\,\mathrm{kg/min}$.

	conventional			SLM		
	$\dot{m}$ [kg/min]	θ [°]	*SMD* [µm]	$\dot{m}$ [kg/min]	θ [°]	*SMD* [µm]
Nozzle (A)	13.8	36.9	184	10.9	36.5	202
Nozzle (B)	8.1	43.6	174	9.7	39.5	218
Nozzle (C)	–	–	–	11.2	34.8	179

Validation
Both experiment and simulation show the same trend between the three different nozzle types. Comparing Table 1 with Table 2 one can see that nozzle (C) always has the highest mass flow, followed by (A) and (B). The simulations with a hydraulically smooth wall underestimate the mass flow, while the simulations with $\varepsilon = 146.6\,\mu\mathrm{m}$ overestimate it, which suggests that the actual roughness should lie between those two values. In general the mass flow is represented appropriately, though.
The spray angle θ gets overestimated in the simulations by about 2%, which is a good agreement.

Conclusions and Outlook
It has been shown that conventional nozzles for a desuperheater can be produced by SLM, even though the printed nozzles generate larger droplets. Nozzle (C), which was designed particularly for SLM, performed better than the other printed nozzles and comparable to the conventional ones. A comparison of several simulations and measurements showed that a high surface roughness increases the mass flow, but also increases the droplet diameter. As a pure VOF simulation cannot predict droplet sizes with a reasonable effort, one would have to use a correlation to calculate the SMD or perform a simulation with VOF to DPM coupling to estimate the droplet size without measurements.
To estimate the SMD of a scaled nozzle a correlation was introduced and the exponent found by measurements showed good agreement with the literature. Surprisingly, the scaling depends strongly on the differential pressure over the nozzle.
With the new information about surface roughness and scaling the nozzle (C) will be optimized by simulations or by measurements. The goal will be to get the most out of the benefits from the new design-freedom.

Acknowledgements
Fruitful discussions with Alexey Denisov are gratefully acknowledged.
Funding from Innosuisse under contract 27938.1 PFIW-IW is also acknowledged.

Nomenclature

A_0	Orifice area [mm^2]	Δp	Pressure difference [MPa]
c_D	Discharge coefficient [–]	ε	Sand grain roughness [µm]
d	Droplet diameter [µm]	θ	Spray angle [°]
d_0	Orifice diameter [mm]	μ_L	Liquid viscosity [µPa s]
$\dot{m}$	Liquid mass flow rate [kg/min]	ρ_A	Air density [$\mathrm{kg/m}^3$]
R_a	Arithmetic average roughness [µm]	ρ_L	Liquid density [$\mathrm{kg/m}^3$]
SMD	Sauter mean diameter [µm]	σ	Surface tension coefficient [mN/m]
t	Film thickness [mm]		
X	Average volume fraction at the orifice [–]		
x	Scaling exponent [–]		

References

[1] Jones A. R., 1982, 2nd International Conference on Liquid Atomization and Spray Systems, Madison, WI (USA).
[2] Adams T., Grant C., Watson H., 2012, "A Simple Algorithm to Relate Measured Surface Roughness to Equivalent Sand-grain Roughness". International Journal of Mechanical Engineering and Mechatronics, Vol. 1, No. 1, pp. 66-71.
[3] Wang, X. F., Lefebvre A. H., 1987, "Mean Drop Sizes from Pressure-Swirl Nozzles". Journal of Propulsion and Power, Vol. 3, No. 1, pp. 11-18.
[4] Benjamin, M. A., Mansour, A., Samant, U. G., Jha, S., Liao, Y., Harris, T., Jeng, S. M., 1998, The American Society of Mechanical Engineers, 98-GT-537.
[5] Jasuja A. K., 1979, "Atomization of crude and resudual fuel oils". Journal of Engineering for Power, Vol. 101, No. 2, pp. 250-258.
[6] Jain M., John B., Iyer K. N., Prabhu S. V., 2014, "Characterization of the full cone pressure swirl spray nozzles for the nuclear reactor containment spray system". Nuclear Engineering and Design, Vol. 273, pp. 131-142.
[7] Lefebvre A. H., McDonell V. G., 2017, "Atomization and Sprays". CRC Press.